Semi-microscopic approach to nucleon-nucleus scattering

Aaina Thapa
Collaborators: Jutta Escher (LLNL)
Emanuel Chimanski (BNL)
Walid Younes (LLNL)
Eunjin In (LLNL)
Sophie Péru (CEA, France)

June 13, 2023
@16th Varenna conference on Nuclear Reaction Mechanisms

LLNL-PRES-850139
This work was performed under the auspices of the U.S. Department of Energy by Lawrence Livermore National Laboratory under contract DE-AC52-07NA27344.
Lawrence Livermore National Security, LLC

Lawrence Livermore National Laboratory

Nucleon-nucleus scattering

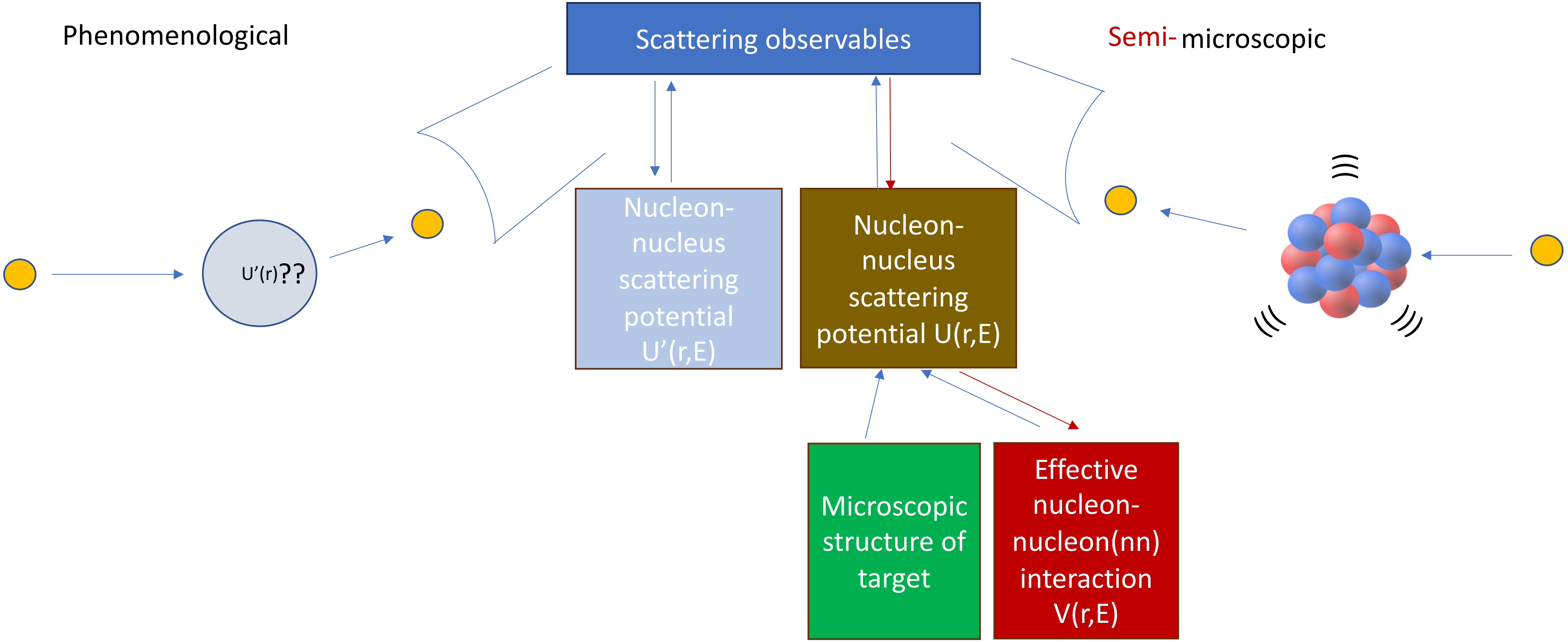

Use nuclear structure of the target nucleus for predictive modelling of nucleon-nucleus scattering

Need for predictive modelling of nucleon-nucleus scattering

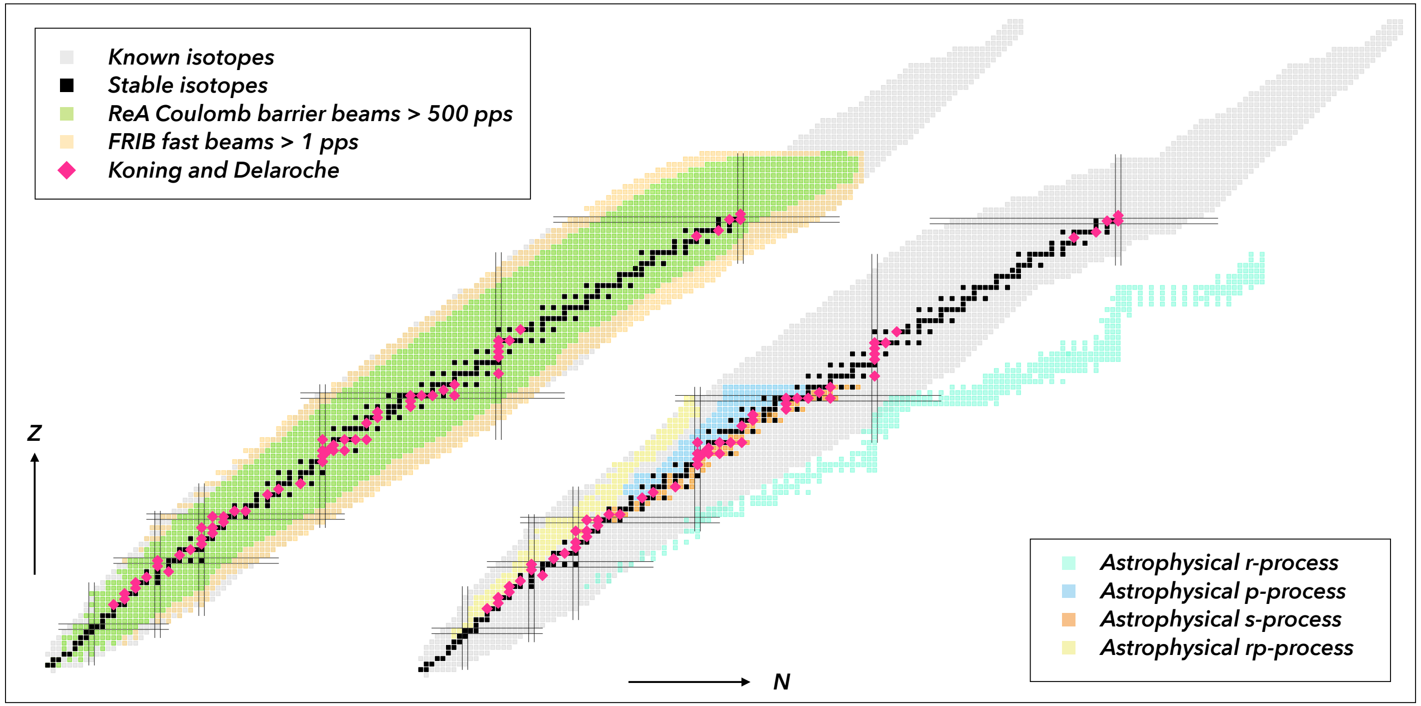

Hebborn, *et al., J. Phys. G: Nucl. and Part. Phys. 50, 060501* (2023)

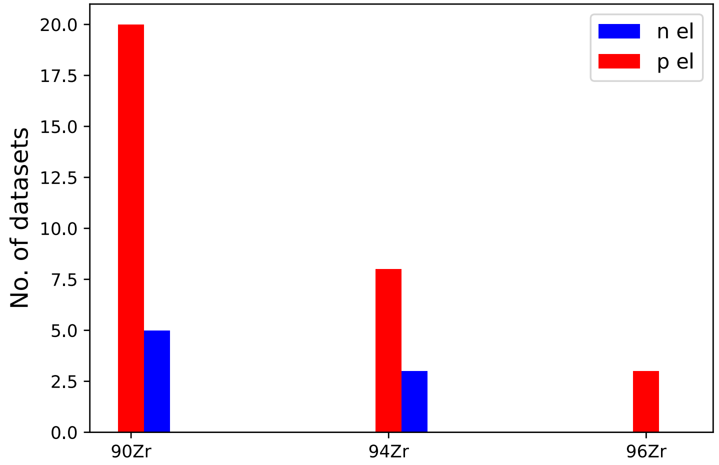

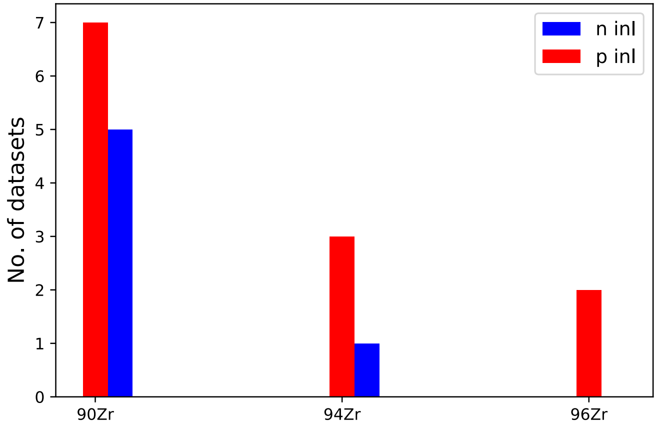

1. Phenomenological optical potentials, like Koning-Delaroche, are fitted to nuclei near stability (LHS).
2. Scattering data is limited as we move to neutron-rich nuclei, neutron-nucleus scattering data is even more scarce (RHS).

Theoretical predictions for nucleon-nucleus scattering cross sections is needed

Microscopic structure of the target nucleus

Calculations done by E. Chimanski ,W. Younes, E. In, J. Escher, S. Peru

Microscopic structure of target

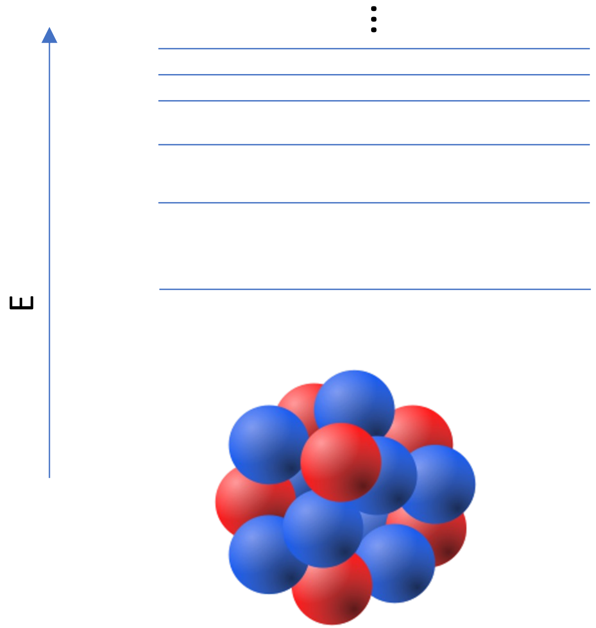

Quasi-random phase approximation (QRPA) method used for vibrational spectrum - two or more nucleons in the nucleus collectively gain energy and excite the nucleus.

+

Hartree-Fock-Bogliubov (HFB) mean-field method for the many-body ground state energy.

Structure properties of $^{98-122}Zr$ using HFB+QRPA (Chimanski, In, Escher, Peru, Younes (to be submitted))

HFB+QRPA many body methods used to calculate ground state and excited states of the nucleus by treating it as an A-body quantum many-body system

Integrating structure and reactions

NN interaction : Gogny D1m interaction

Many-body method : HFB

Ground state energy and wavefunction

Many-body method : QRPA

vibrational excited state energies and transition densities

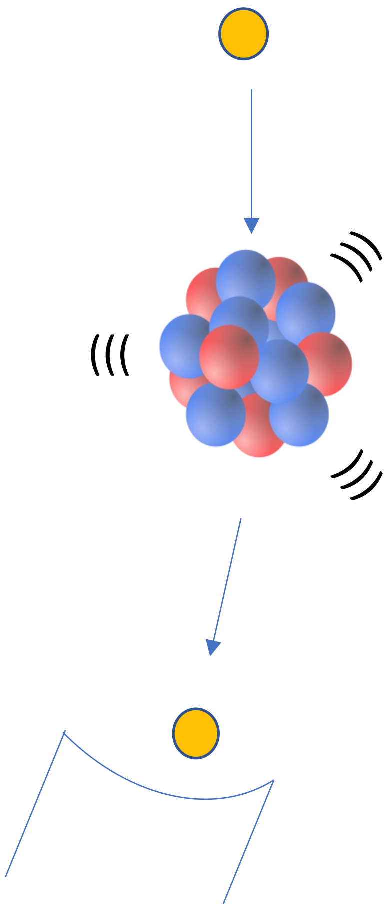

JLM approach

Local energy dependent optical potential

JLM approach

Local energy dependent coupling potentials

$$\left\{\frac{d^2}{dr^2} - \frac{l_c(l_c+1)}{r^2} - \frac{2\mu_c}{\hbar^2}V^{\partial}_{cc}(r) + k_c^2\right\} u_c(r) = \sum_{c'\neq c} \frac{2\mu_c}{\hbar^2} V^{\partial}_{cc'}(r)\, u_{c'}(r),$$

FRESCO

Scattering cross section

Effective nucleon-nucleon interaction : JLM approach

J.P. **J**eukenne, A. **L**ejeune, and C. **M**ahaux, Phys. Rev. C 15, 10 (1977).

Effective nucleon-nucleon(NN) interaction V(r,E)

Hard core Reid's NN interaction → Brueckner-Hartree-Fock → Medium effects : Parametrized NN interaction in nuclear matter → Improved local density Approximation (ILDA) + single-folding (i.e. integrate over all **r'**) → Nucleon- nucleus potential at positive energies: Nuclei are finite with density varying spatial density

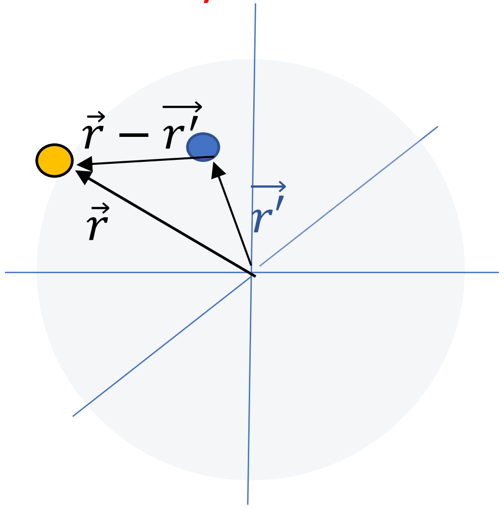

1. The parameters are fitted to reproduce the on-shell g-matrix in infinite nuclear matter (under Bruekner-Hartree-Fock approximation), with bare nucleon-nucleon interaction as hard-core Reid's interaction.

$$\mathrm{Re}(V_{nn}^{NM}(\rho,E)) = \sum_{ij} a_{ij}\rho^i E^{j-1} + \alpha \sum_{ij} b_{ij}\rho^i E^{j-1}$$

$$\mathrm{Im}(V_{nn}^{NM}(\rho,E)) = \left[1+\frac{D}{(E-\epsilon_F)^2}\right]^{-1} \sum_{ij} d_{ij}\rho^i E^{j-1} + \alpha\left[1+\frac{\mathrm{F}}{\mathrm{E}-\epsilon_F}\right]^{-1} \sum_{ij} f_{ij}\rho^i E^{j-1} \quad \text{-- (1)}$$

2. The parameterized in-medium **nucleon-nucleon** interaction has the form

$$V_{nn}^{JLM}(\rho\,,E) = V_0(\rho,E) + iW_0(\rho,E) + \alpha[V_1(\rho,E\,) + W_1(\rho,E)],\ \alpha = \frac{\rho_n-\rho_p}{\rho_n+\rho_p}$$

3. Finite-range effects : Finite nucleus has non-uniform density over the range of interaction.

JLM model parametrizes the in-medium NN interaction at positive energies in infinite nuclear matter.

JLM approach : 1977 to present

JLM version	Energy	Nuclei	Quantity reproduced	Variations studied	LImitations
Original JLM – 1977 (jeukenne, Lejeune and Mahaux)	1 MeV <= E <= 160 MeV	**tested for** : ^{12}C, ^{16}O, ^{27}Al, ^{40}Ca, ^{58}Ni, ^{120}Sn, ^{208}Pb	a. Volume Integrals b. mean-square radius of OMPs.	a. LDA (gave smaller OMP mean square radii) b. ILDA	a. Limited to E<=160 b. separate parameters below 10 MeV c. no spin-orbit
Semi-microscopic - 1998 (Eric Bauge et al.)	1 MeV <= E <= 200 MeV	**fit to** : ^{40}Ca, $^{54,56}Fe$, $^{58,60}Ni$, $^{63,65}Cu$, ^{90}Zr, ^{93}Nb, $^{116,120}Sn$, ^{208}Pb, ^{209}Bi	a. +Differential elastic cross section b. + Analyzing power	a. Several ILDA b. different b. spin-orbit prescriptions c. HFB density+D1M	a. Weak iso vector components.
Lane consistent - 2001 (JLM-B) (Eric Bauge et al.)	1 keV <= E <= 200 MeV	**fit to: +** ^{48}Ca, ^{70}Zn, ^{96}Ru, $^{61,62,64}Ni$, ^{96}Zr, $^{96,92}Mo$, ^{115}In, ^{93}Nb $^{112,116,117\text{-}119,124}Sn$, ^{104}Pd, ^{138}Ba, ^{142}Nd, ^{144}Sm	a. + Quasi elastic (p,n) differential cross section b. + analyzing power		

JLM-B : $V_{nn}^{JLM}(\rho, E) = \lambda_{v_0}[V_0(\rho,E) \pm \alpha\lambda_{V_1}V_1(\rho,E)] + i\lambda_{W_0}[W_0(\rho,E) \pm \alpha\lambda_{W_1}W_1(\rho,E)] + S.O\,(\lambda_{V_{SO}}, \lambda_{W_{SO}})$.

, + for incident neutron, - for incident proton

JLM model as we use today is semi-microscopic, the renormalization factors or the $\lambda\,'s$ are fit to scattering data.

Optical potential : JLM-B v.s. Koning Delaroche

JLM-B

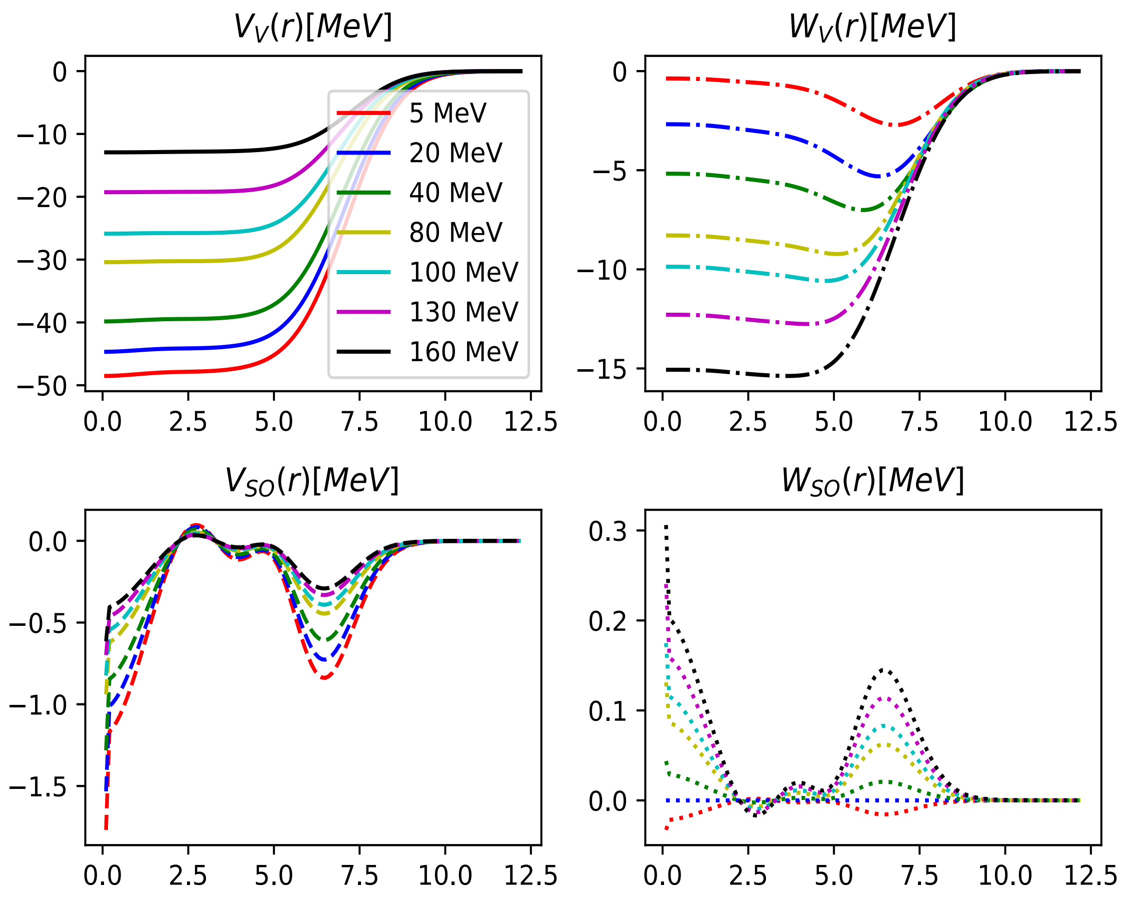

KD

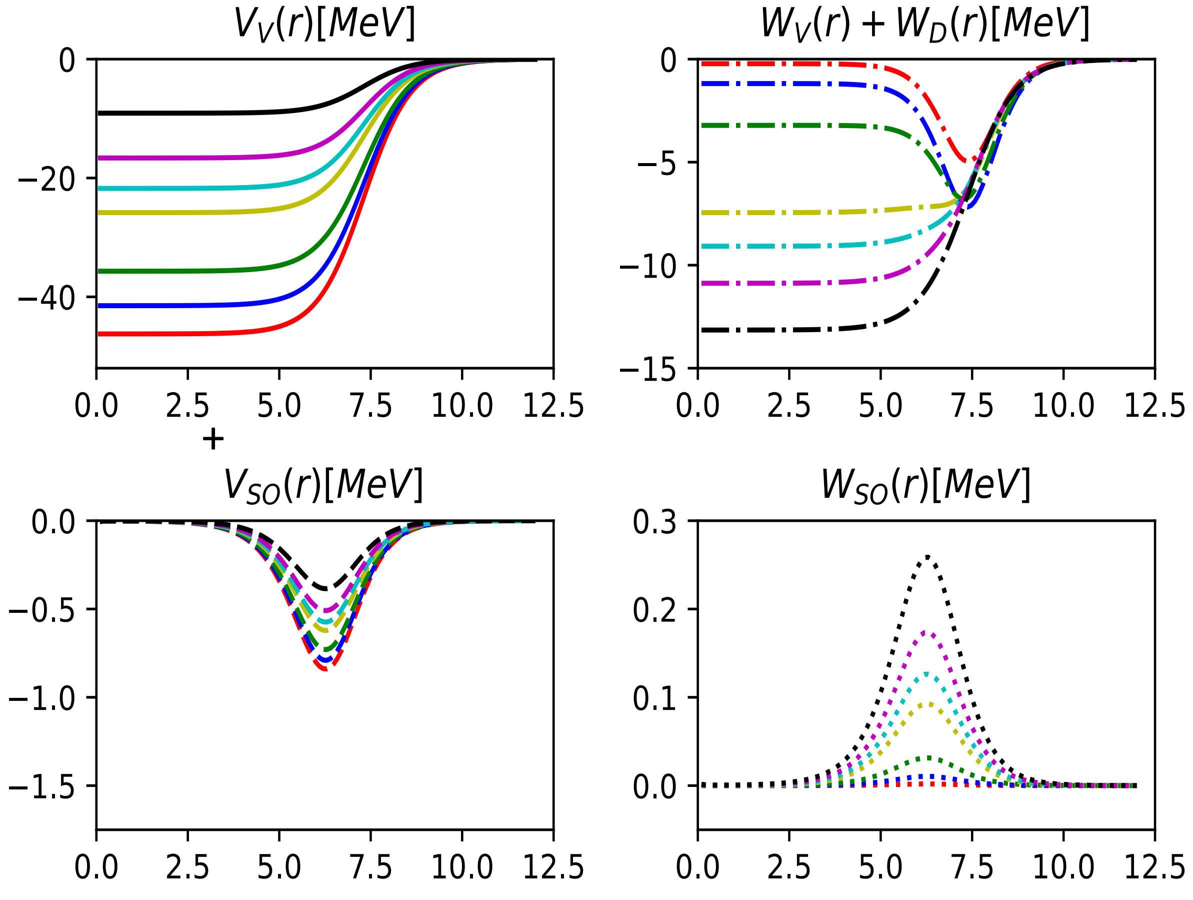

n – 208Pb case, the central imaginary term includes surface term as well

Semi-microscopic JLM-B. vs phenomenological Koning-Delaroche model for 208Pb(n,n)

JLM for inelastic scattering (Lagrange et al. 1983, Cheon et al. 1985, Dupuis et al. 2015)

$$\left\{\frac{d^2}{dr^2}-\frac{l_c(l_c+1)}{r^2}-\frac{2\mu_c}{\hbar^2}V_{cc}^{\partial}(r)+k_c^2\right\}u_c(r)=\sum_{c'\neq c}\frac{2\mu_c}{\hbar^2}V_{cc'}^{\partial}(r)\,u_{c'}(r),$$

The goal is to calculate need to calculate coupling potentials

1. Effective JLM interaction : density-dependent interaction -> During inelastic scattering when target get excited, target density changes.

2. The transition densities gives us information about the change in target density after the target is excited.

3. Contribution from the variation of effective interaction as the transition happens : Rearrangement term.

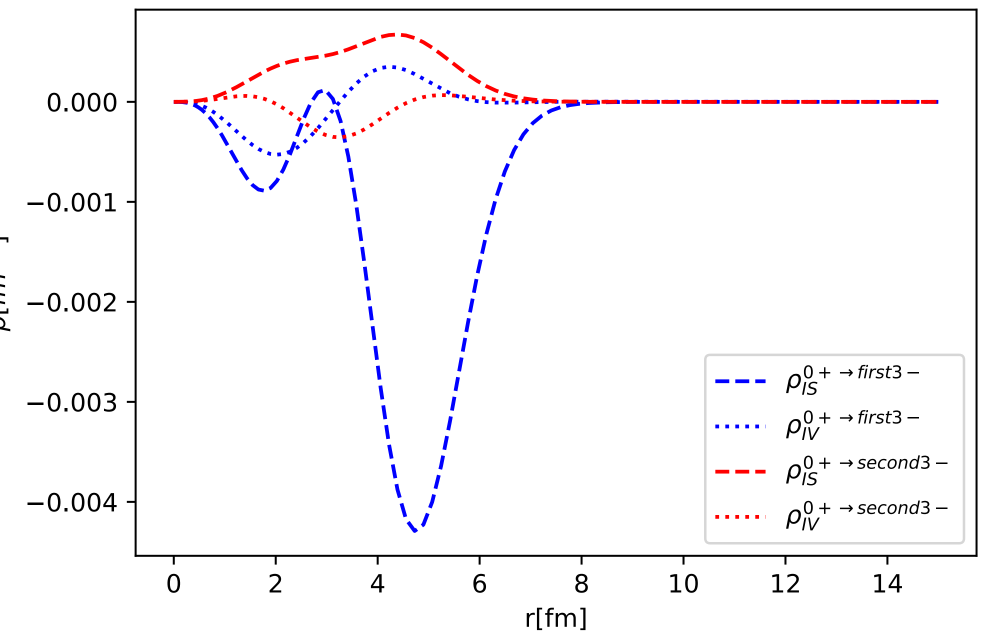

Transition density for first two 3- states in 90Zr from Gogny D1m+ QRPA

So, Full coupling potential calculated using, $\rho_{tr}\, V_{nn}^{JLM}(\rho,E)+\boldsymbol{\rho_{tr}\rho_0}\,\frac{\boldsymbol{dV_{nn}^{JLM}(\rho,E)}}{\boldsymbol{d\rho}}$

Results : Elastic scattering using JLM method

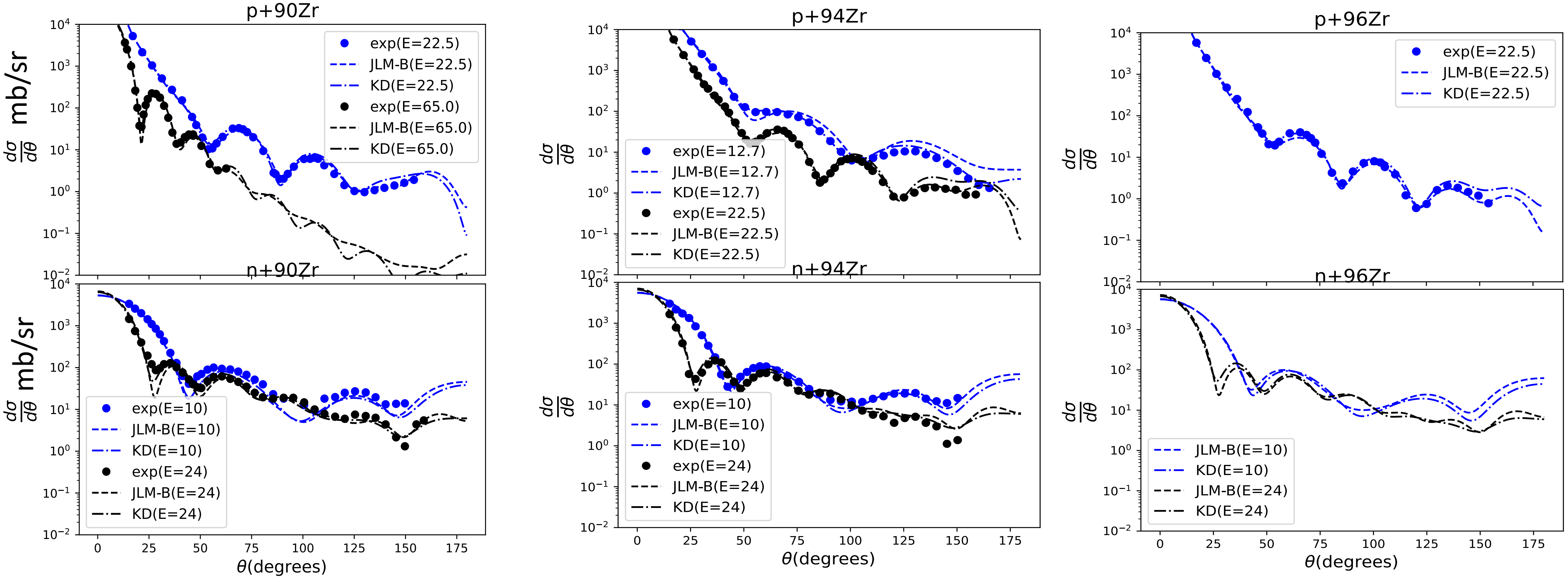

1. Good agreement with measured cross sections (dots) for 90,94 and 96Zr.
2. Compares well to much used phenomenological Koning-Delaroche nucleon-nucleus potential.

For elastic scattering method works well, next we use the same in-medium NN interaction for inelastic scattering.

Neutron inelastic scattering : 90Zr(n, n')

First 3-

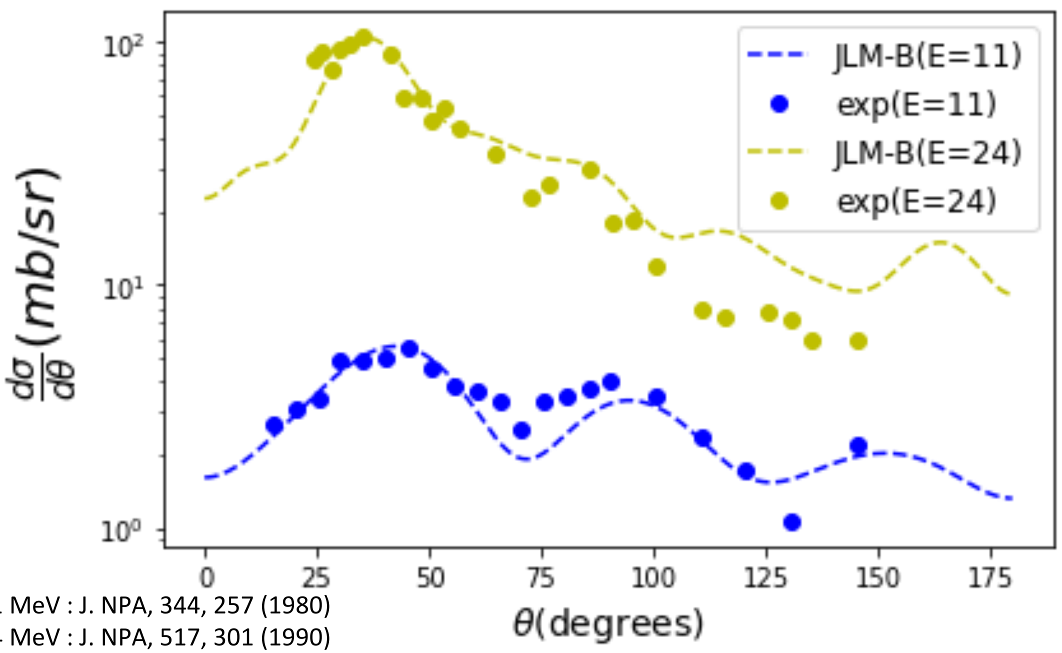

At 11 MeV : J. NPA, 344, 257 (1980)
At 24 MeV : J. NPA, 517, 301 (1990)

First 2+

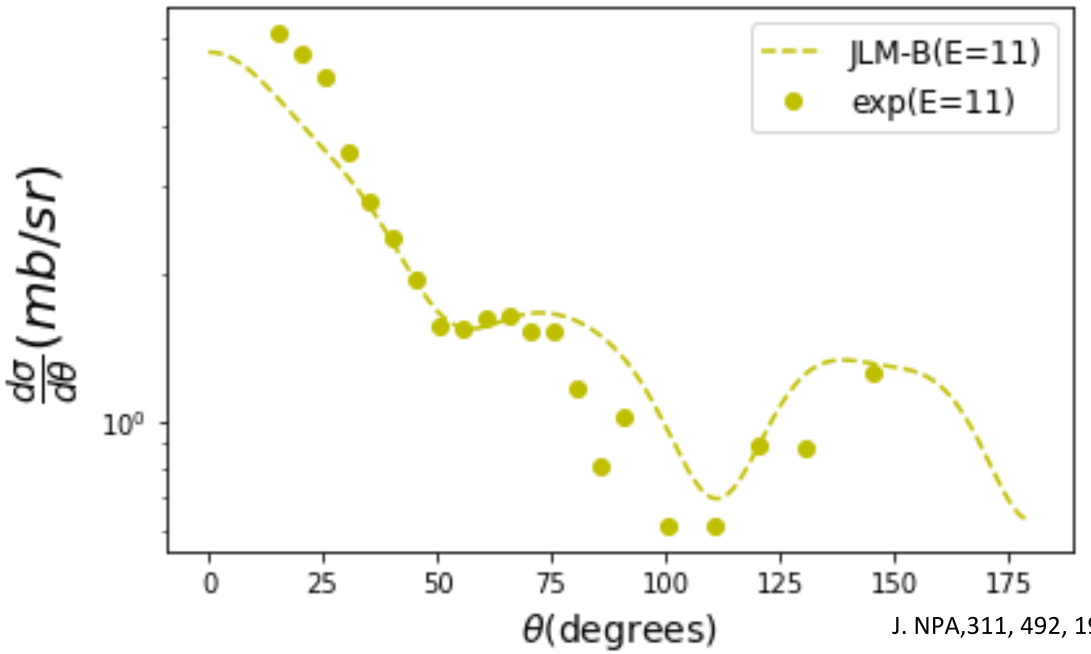

J. NPA,311, 492, 197812 (1978)

Proof-of-principle inelastic scattering calculations for 90Zr(n,n') are encouraging

Inelastic scattering : 90Zr(p,p') at 25 MeV

$J^\pi = 2^+$

E(QRPA)	E(exp) (Bijl1983)
2.725	2.185
3.237	3.311
4.039	3.846

Isotope	$E(2^+)$ (MeV)	QRPA (e^2b^2)	Exp (e^2b^2)	QRPA (WU)	Exp (WU)
^{90}Zr	2.186	0.0311	0.0610	2.6	5.1
^{96}Zr	1.750	0.0995	0.055, 0.0314	7.6	4.2, 2.41

$J^\pi = 3^-$

E(QRPA)	E(exp)
2.85	2.751
4.98	4.5

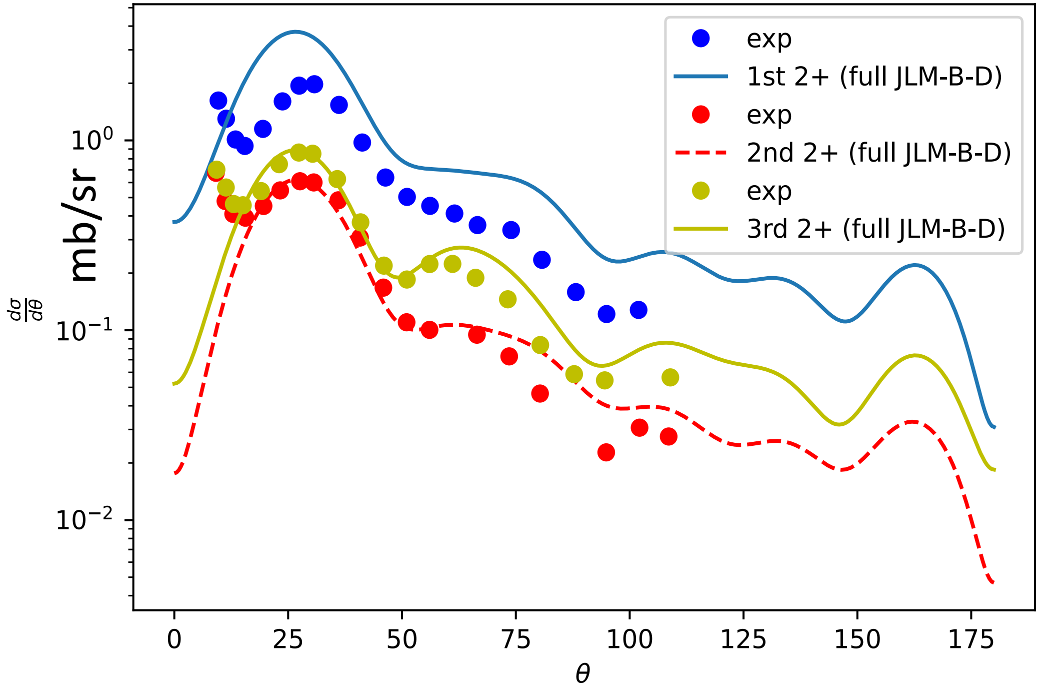

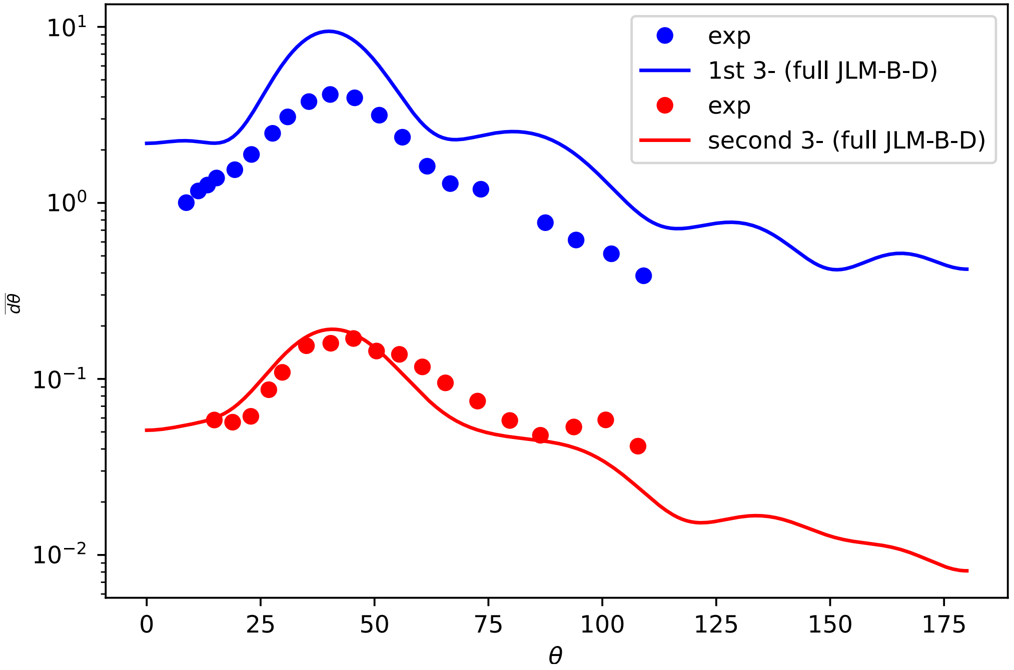

Using distorted Bonn-wave approximation (DWBA) ie., only including transitions from ground state to excited states.

Preliminary differential cross section results for 90Z(p,p') to first three 2+ and first two 3- excited states for 90Zr.

Effect of Coulomb contribution to coupling potentials?

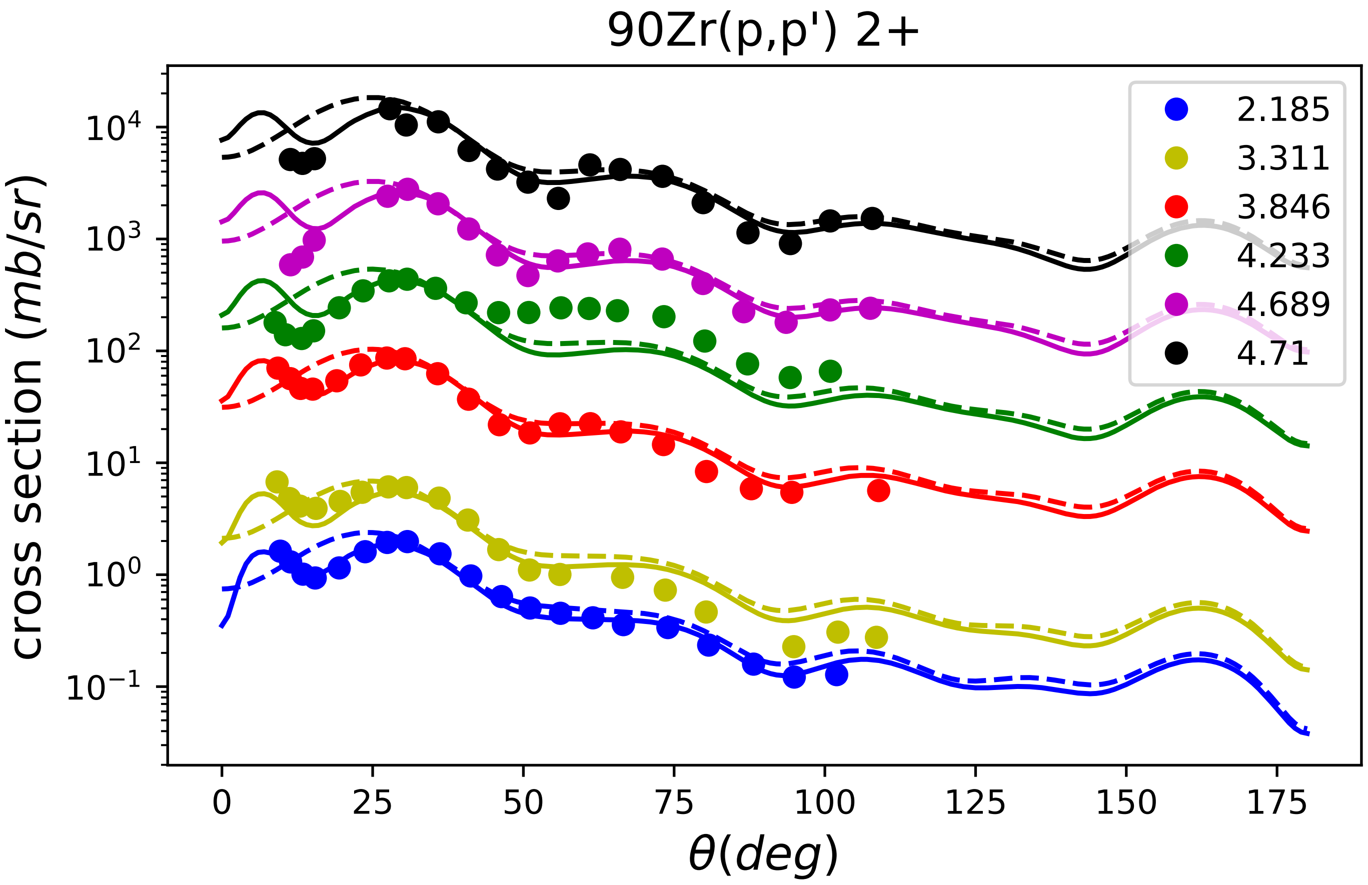

Dashed curve : No Coulomb added to transition potential from Collective model

Solid curve : Collective model with Coulomb contribution to transition potentials

Dots : Experimental results

Coulomb contribution in transition potential causes the uptick in differential cross section in Collective Model -> We need to Implement Coulomb contribution to the transition potential

Charged-particle nucleus scattering: Neutron capture cross section using surrogate

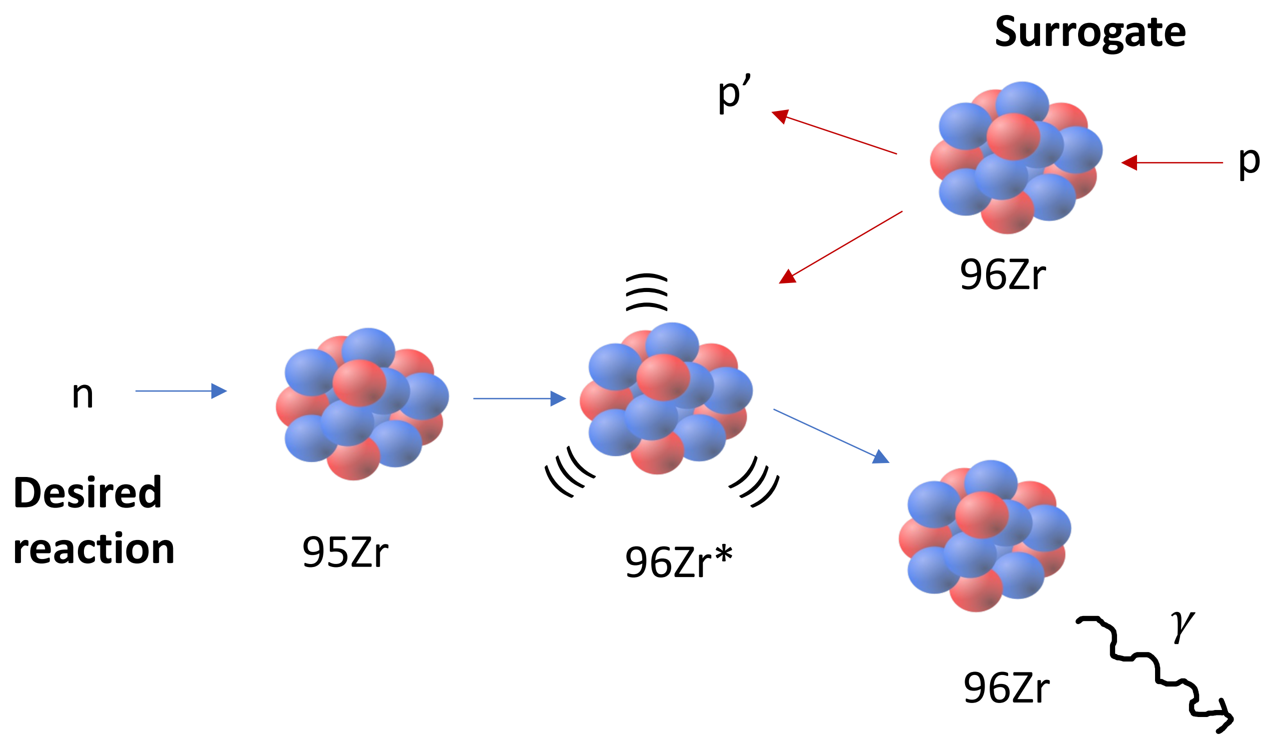

Will be calculated using this work
Angle integrated cross sections as a function of energy for a given spin J and parity π.

A Surrogate experiment gives

$$P_{(p,p'\gamma)}(E) = \sum_{J,\pi} F_{(p,p')}^{CN}(E,J,\pi) \cdot G^{CN}_{\gamma}(E,J,\pi)$$

$^{90}Zr(n,\gamma)$ cross section:

$$\sigma_{(n,\gamma)} = \sum_{J,\pi} \sigma_{n+target}^{CN}(E,J,\pi) \cdot G^{CN}_{\gamma}(E,J,\pi)$$

Concept: Escher *et al*, RMP 84 (2012) 353; EPJConf 122 (2016) 12001

Fig. from J. Escher

Inelastic scattering can be used as a surrogate reaction to predict neutron capture cross sections for unstable nuclei

Outlook

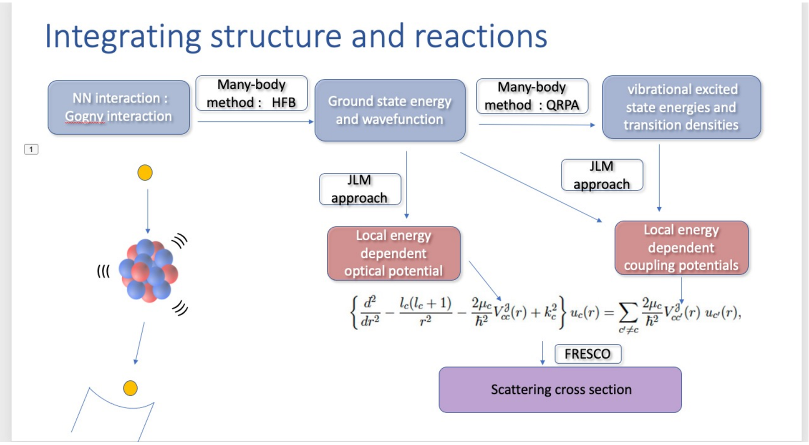

1. Inelastic scattering cross section calculations for 94Zr, 96Zr and 96Mo.

2. Study the impact of structure and NN interaction modelling individually on scattering cross sections and investigate ways to improve the JLM method.

3. Near-term surrogate applications to calculate neutron capture cross section for 95Zr and 95Mo : Generate spin-distributions for 96Zr(p,p’), and 96Mo(p,p’).

4. Implement JLM approach for deformed nuclei.

A thank you to my collaborators:

LLNL: J. Escher, E. In, W. Younes,
BNL/NNDC: E. Chimanski
CEA/France: S. Péru

And admin support:

LLNL: L. Frazier

Summary

1. Developing capability to connect nuclear structure with nucleon-nucleus scattering cross sections.

2. We implemented JLM approach to this end.

3. For elastic scattering, we get good agreement with phenomenological models

4. Preliminary results for inelastic scattering were presented, checks are underway.

5. The applications of interest : use inelastic scattering as surrogate reaction for predicting neutron-capture cross sections

A thank you to my collaborators:

LLNL: J. Escher, E. In, W. Younes,
BNL/NNDC: E. Chimanski
CEA/France: S. Péru

And admin support:

LLNL: L. Frazier

Extras – Structure Results

90Zr : Structure methods vs Experiments

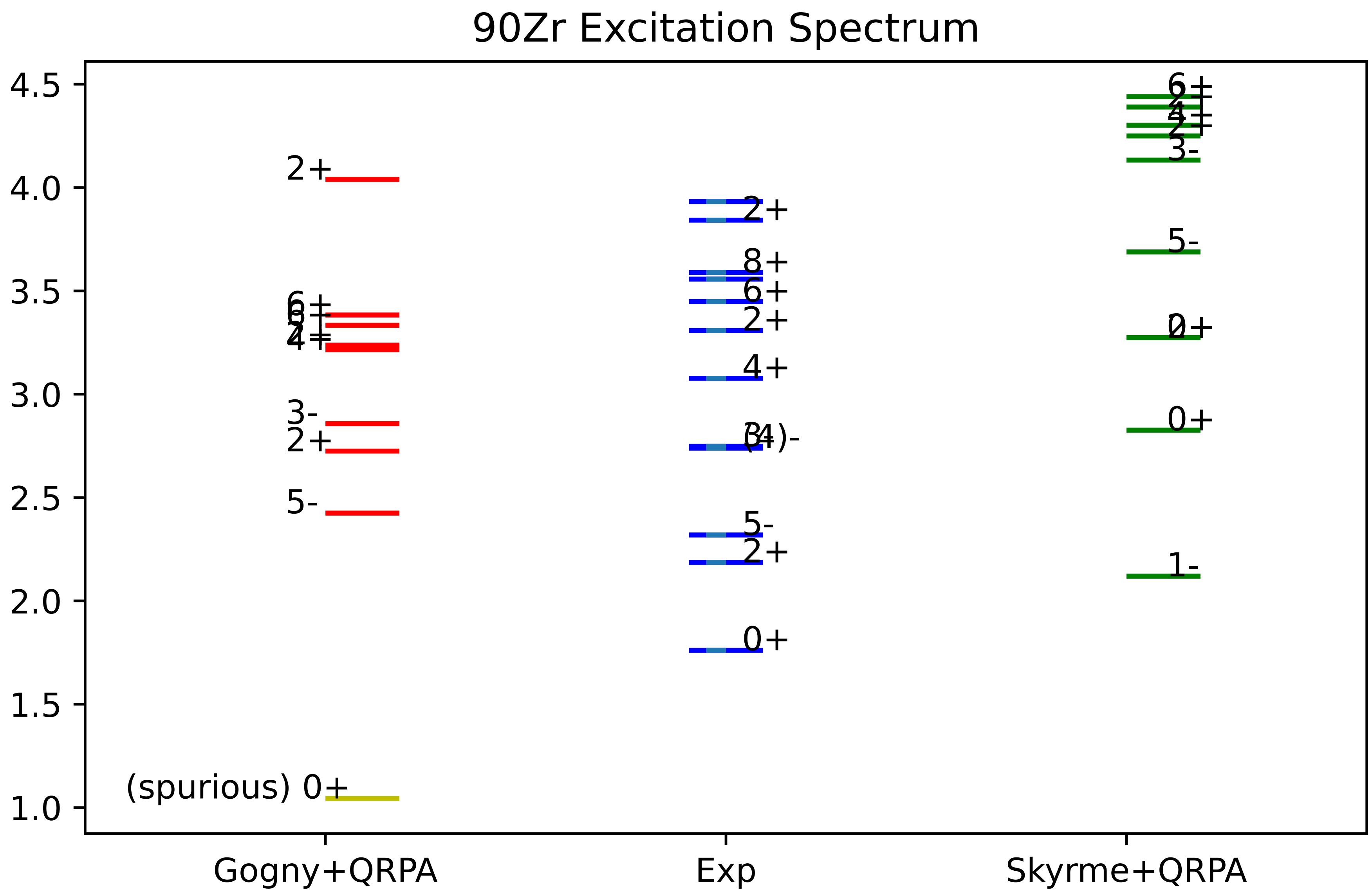

94Zr and 96Zr spectrum from QRPA

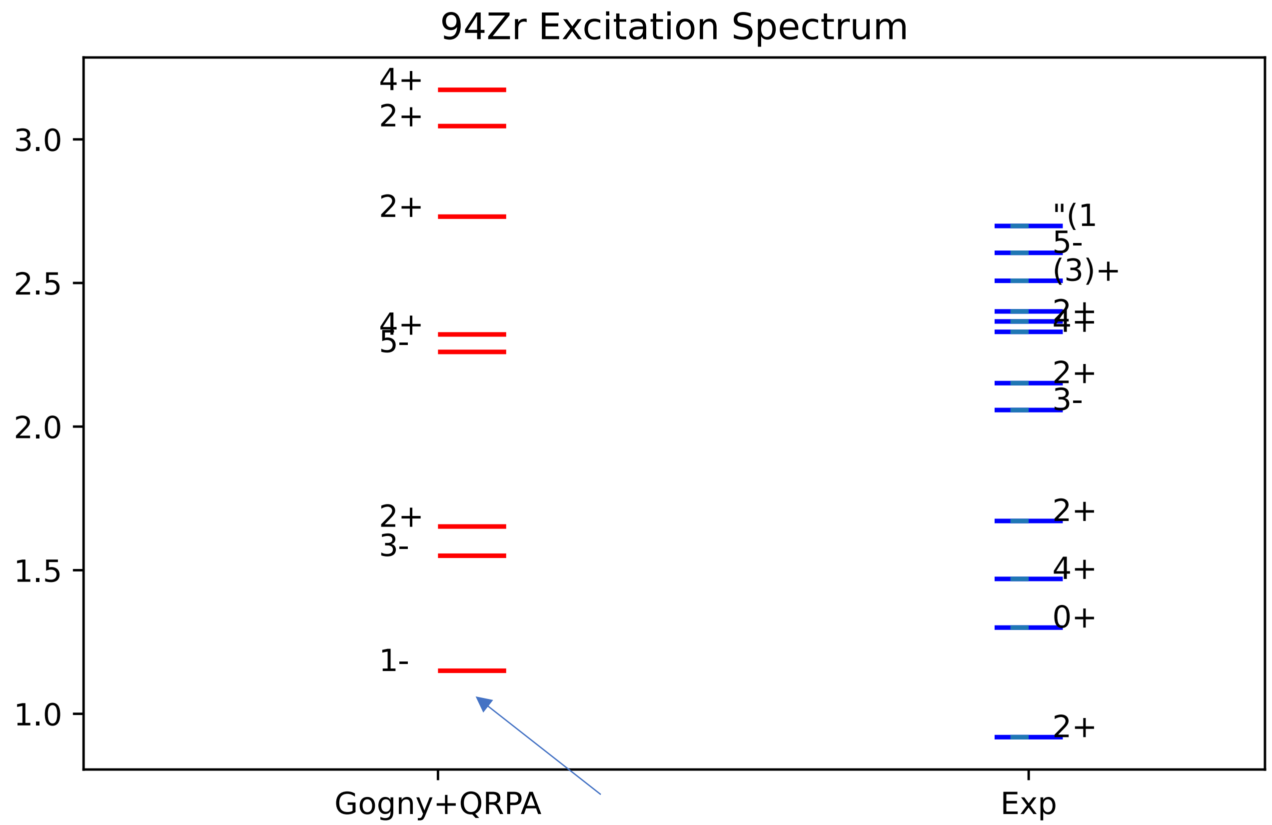

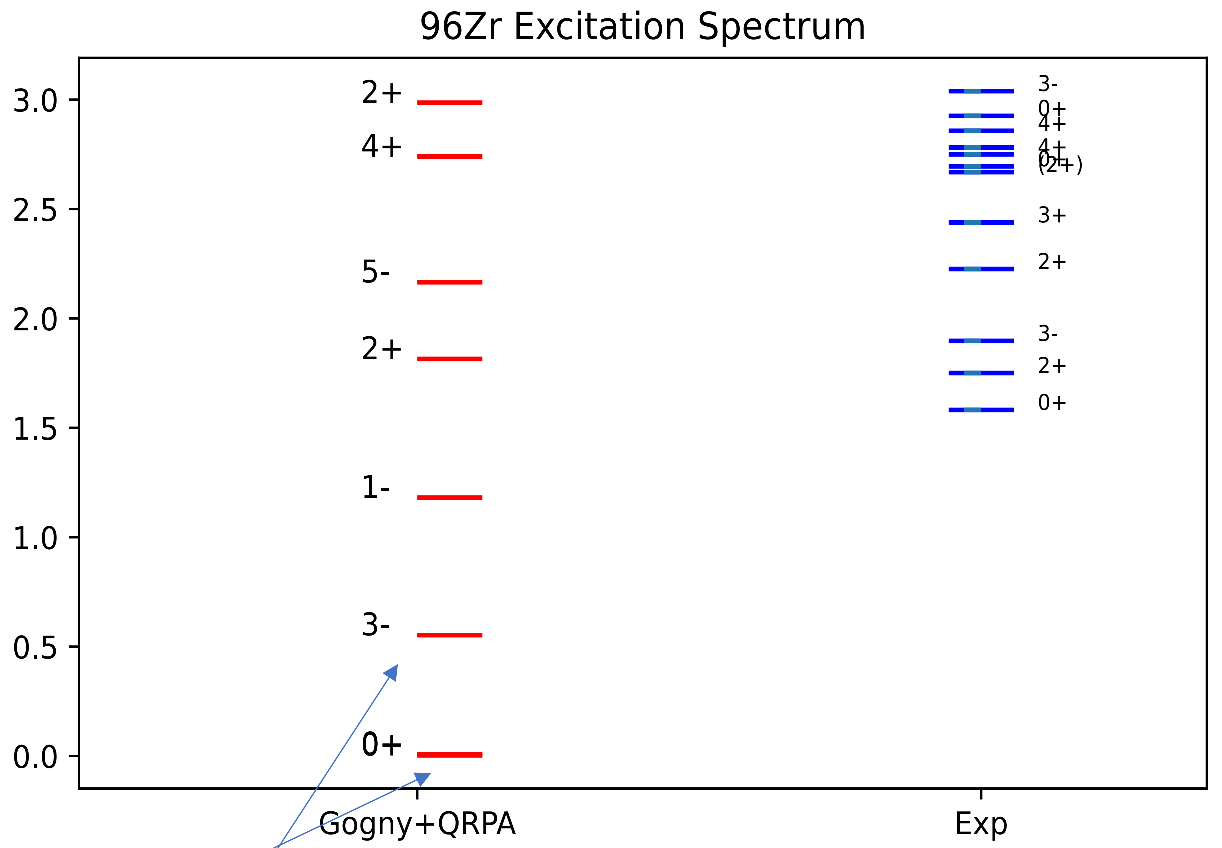

1.14993179	1	0.36916554	n=1_radial_J=1_K=0.dat

0.00314798	0	5.00E-05	n=1_radial_J=0_K=0.dat
0.00792084	0	2.63E-06	n=2_radial_J=0_K=0.dat
0.55259675	3	0.44245028	n=1_radial_J=3_K=0.da

Spurious states

Structure predictions from HFB: ground state properties of the Zr isotopes

Chimanski, In, Escher, Peru, Younes (to be submitted)

Energy as function of β

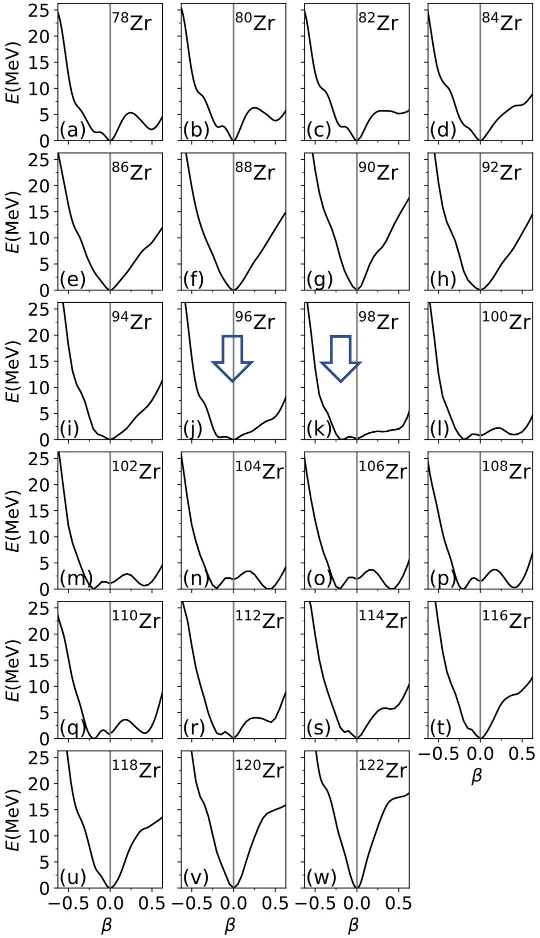

Gogny D1M interaction
Axially-symmetric deformed basis
11 oscillator shells

Binding energies/two-neutron separation energies

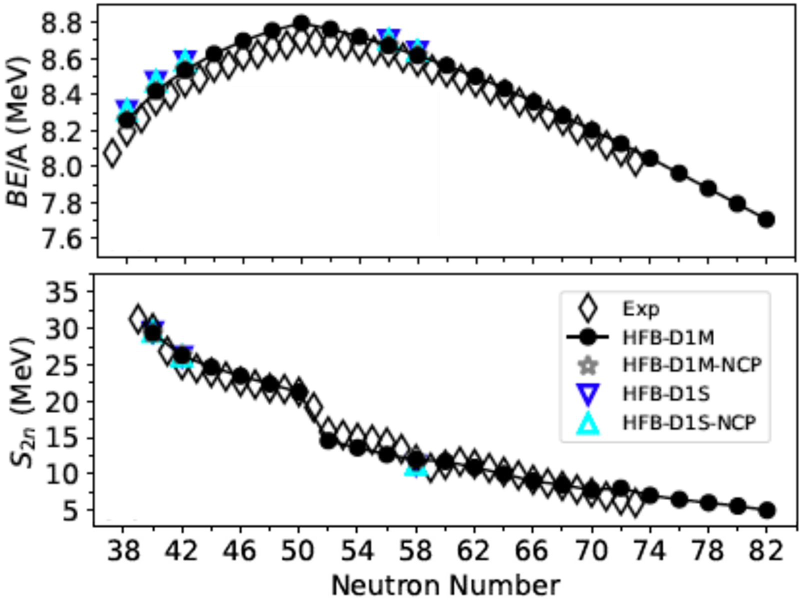

Shape Evolution of ground state Zr isotopes:

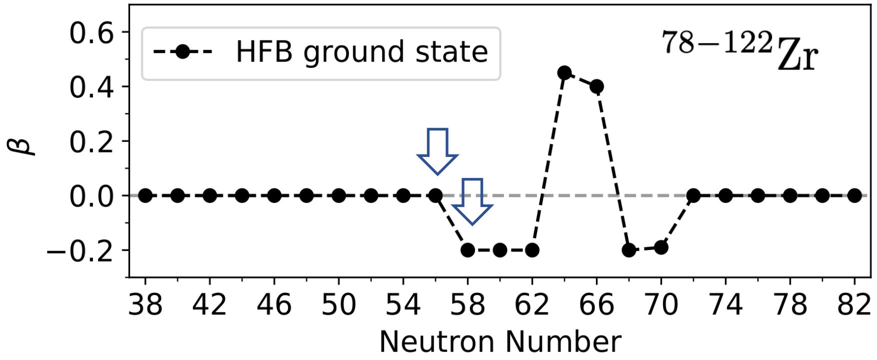

HFB isotopic charge radius shifts

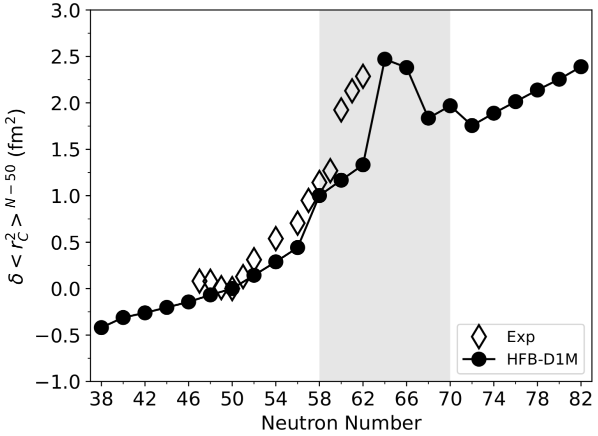

Slide from J. Escher

Predicted systematics agree well with experiment - with some exceptions

Structure predictions from HFB: ground state properties of the Zr isotopes

Chimanski, In, Escher, Peru, Younes (to be submitted)

Energy as function of β

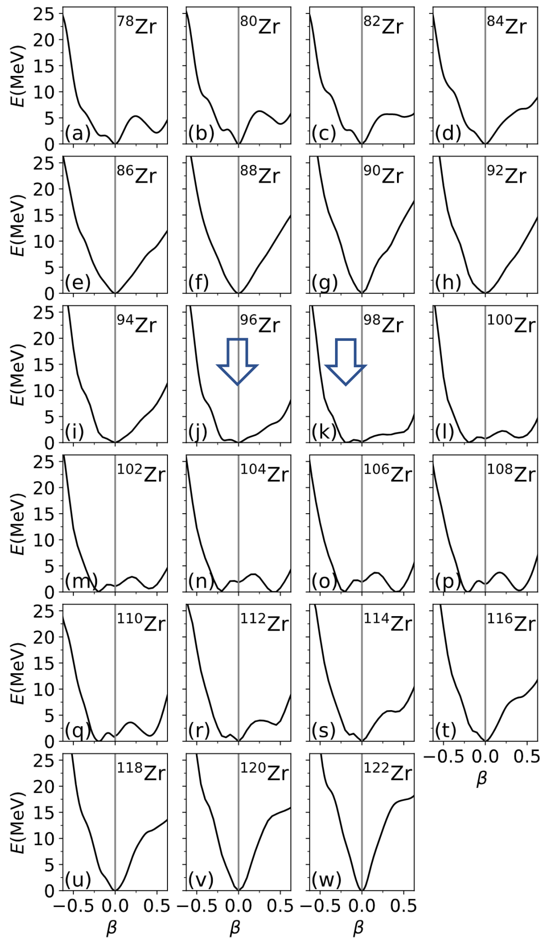

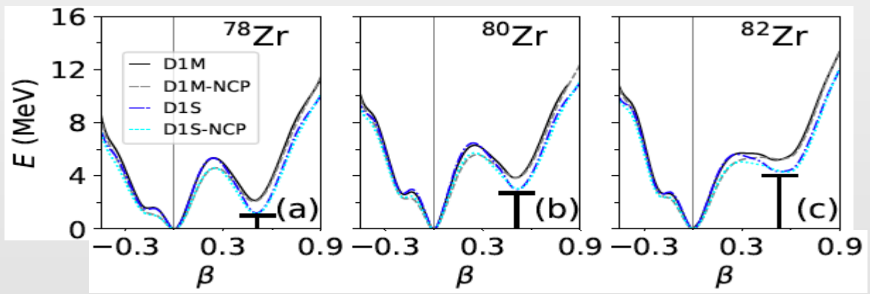

The energy surface is sensitive to approximations used - more robust calculations would allow for mixing.

20-ERD-030

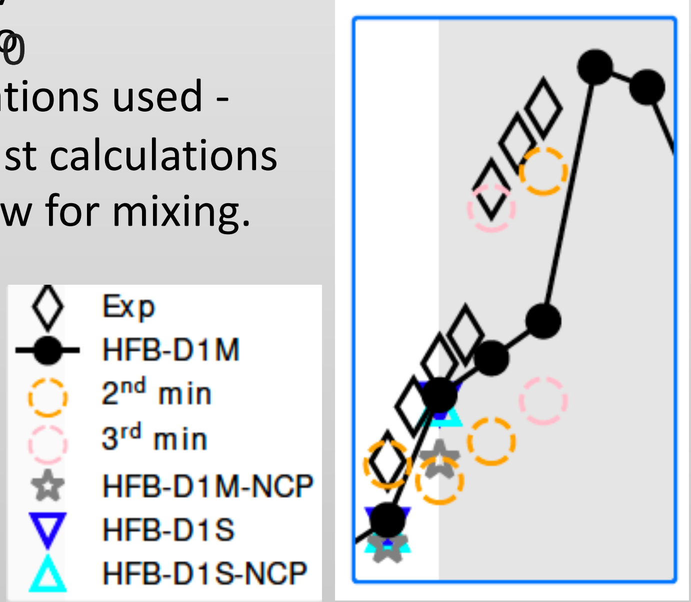

Shape Evolution of ground state Zr isotopes:

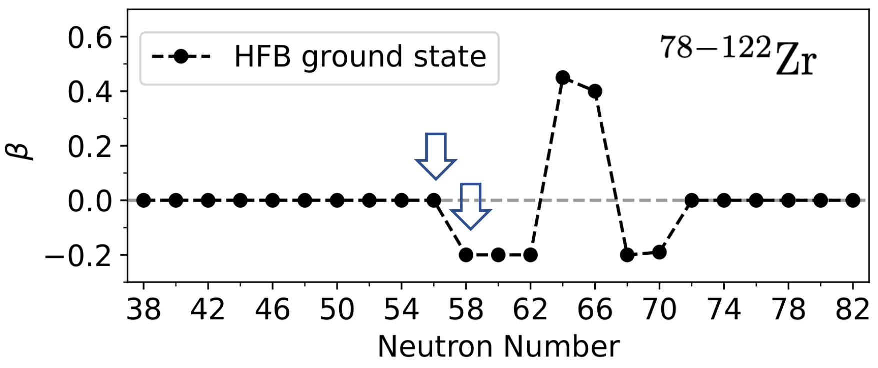

HFB isotopic charge radius shifts

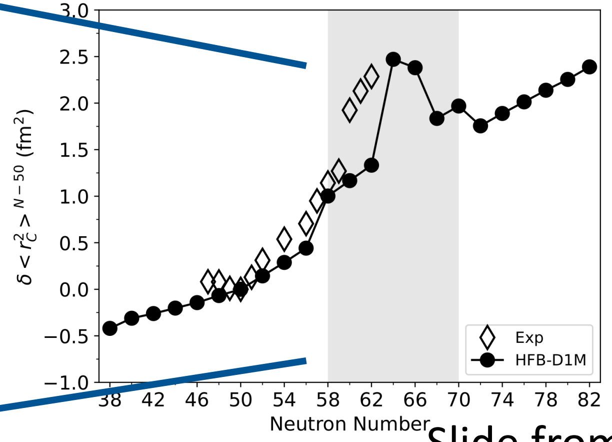

Slide from J. Escher

Discrepancies reveal shortcomings in method or implementation: approximations, interaction,…

Extras – About Scattering

At higher incident energy of E = 185 MeV

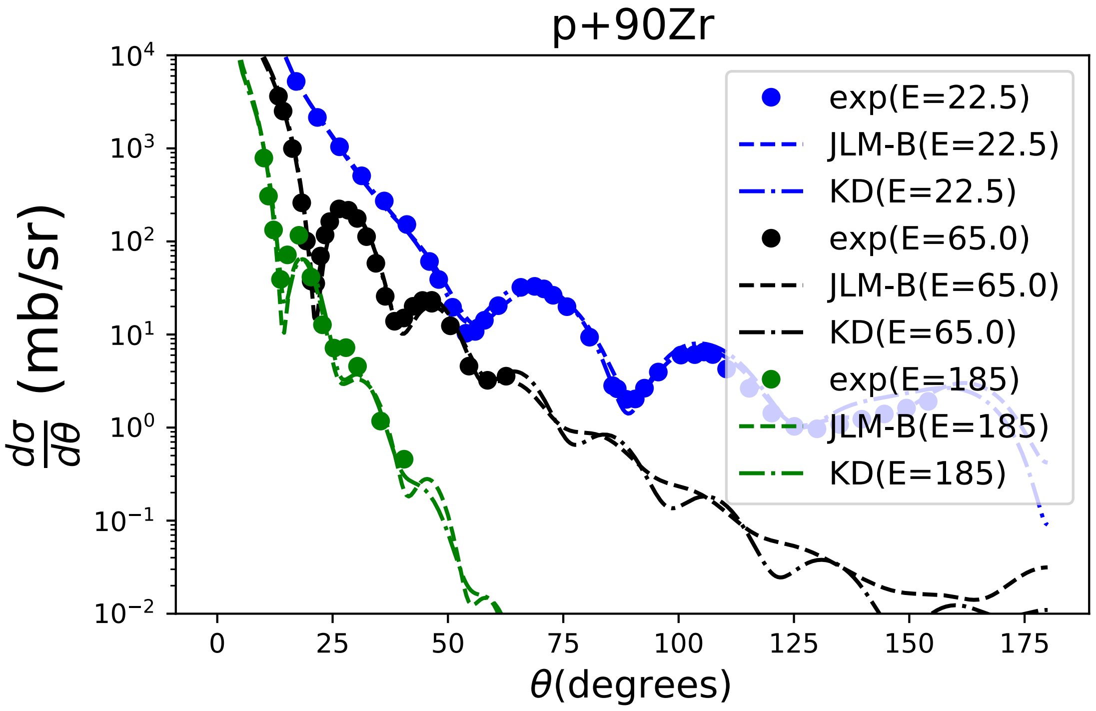

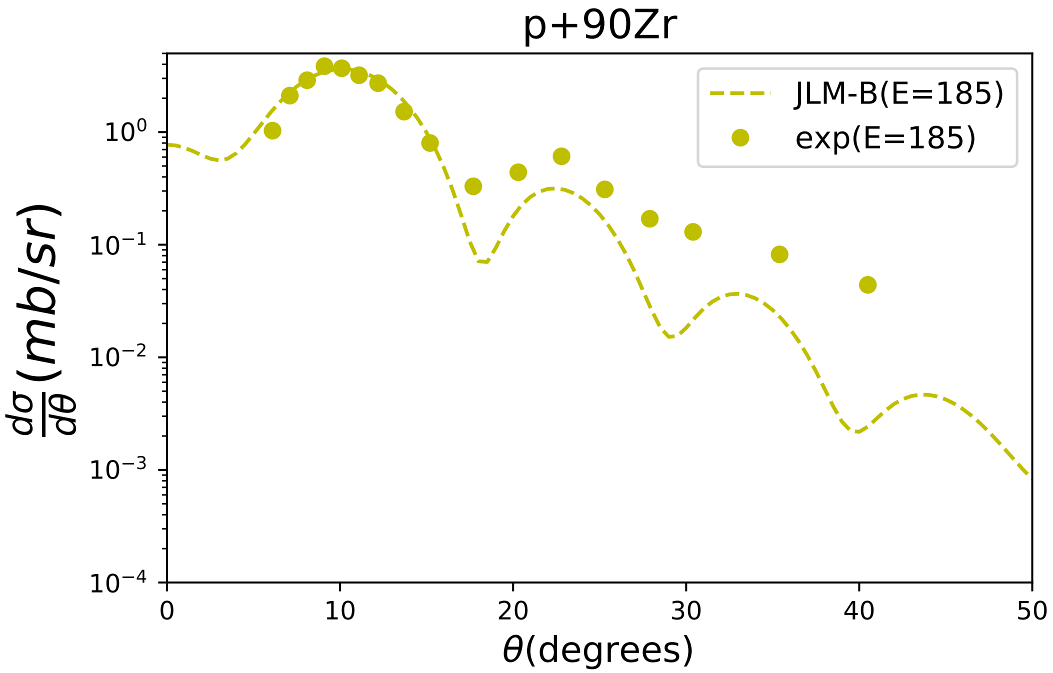

Inelastic scattering : 90Zr(p,p’)

Work in progress

$J^{\pi} = 2^{+}$

E(QRPA)	E_exp (Bijl1983)
2.725	2.185
3.237	3.311
4.039	3.846

Radial Transition Densities : Different colors show different excited states.

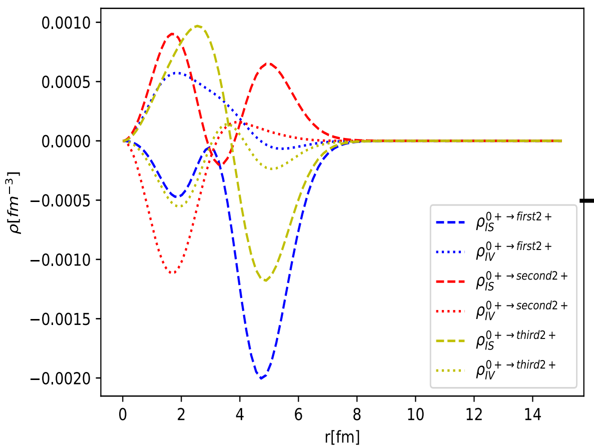

The folded nucleon-nucleus transition potential after folding. Upper panel shows the real part of the potential, lower panel shows the imaginary part.

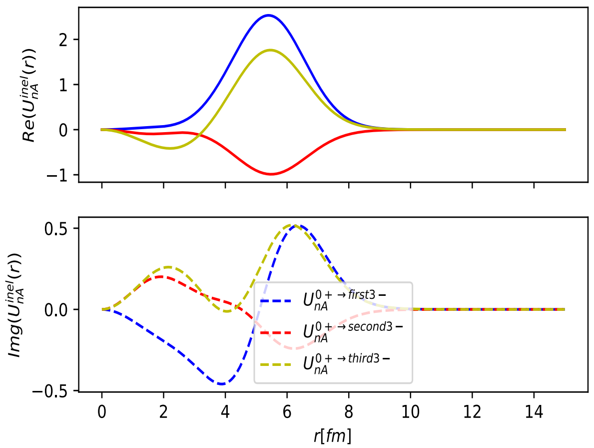

Inelastic differential cross section when target is excited to a particular excited state.

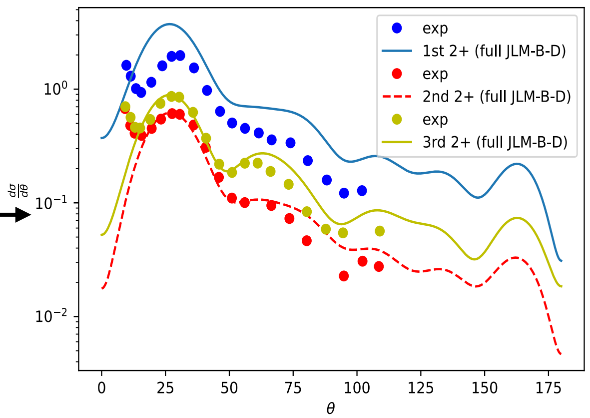

$J^{\pi} = 3^{-}$

E(QRPA)	E_exp
2.85	2.751
4.98	4.5

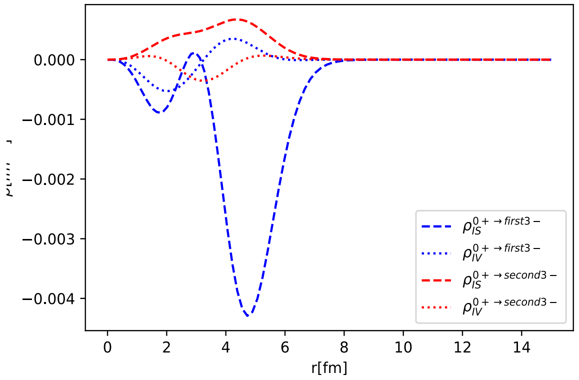

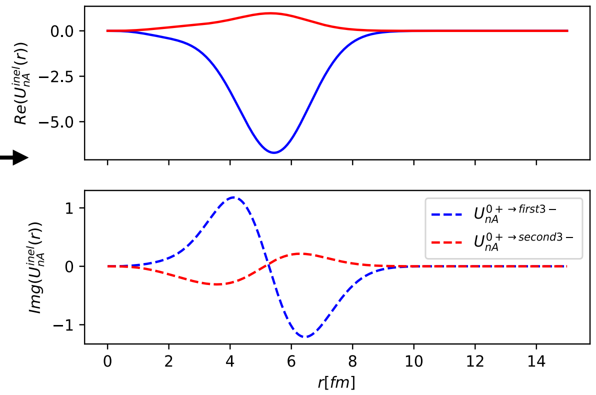

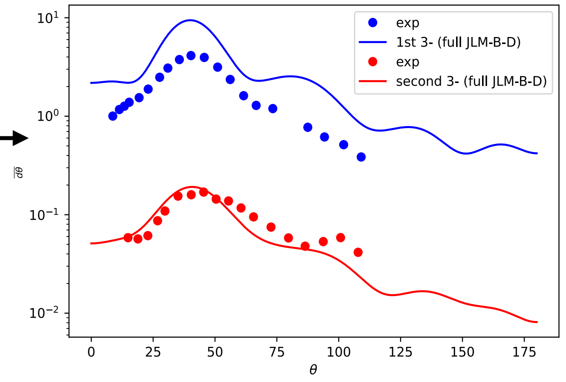

Bauge JLM vs Original JLM [with ti=tr = 1.2] (elastic scattering)